Accepted for publication in Journal of Experimental Marine Biology and Ecology

Morphotypes of the common beadlet anemone *Actinia equina* (L.) are genetically distinct

Running head: mtDNA of *Actinia equina*

Craig S. Wilding[1] and Gareth D. Weedall.

School of Natural Sciences and Psychology,
Liverpool John Moores University,
Liverpool,
L3 3AF.
UK.
1: Corresponding author

Keywords: Cnidaria, sea anemone, beadlet anemone, *Actinia equina*, barcoding, *COI*

Abstract

Anemones of the genus *Actinia* are ecologically important and familiar organisms on many rocky shores. However, this genus is taxonomically problematical and prior evidence suggests that the North Atlantic beadlet anemone, *Actinia equina*, may actually consist of a number of cryptic species. Previous genetic work has been largely limited to allozyme electrophoresis and there remains a dearth of genetic resources with which to study this genus. Mitochondrial DNA sequencing may help to clarify the taxonomy of *Actinia*. Here, the complete mitochondrial genome of the beadlet anemone *Actinia equina* (Cnidaria: Anthozoa: Actinaria: Actiniidae) is shown to be 20,690bp in length and to contain the standard complement of Cnidarian features including 13 protein coding genes, two rRNA genes, two tRNAs and two Group I introns, one with an in-frame truncated homing endonuclease gene open reading frame. However, amplification and sequencing of the standard mtDNA barcoding region of the *cytochrome oxidase 1* gene revealed only two haplotypes, differing by a single base pair, in widely geographically separated *A. equina* and its congener *A. prasina*. *COI* barcoding shows that whilst *A. equina* and *A. prasina* share the common mtDNA haplotype, haplotype frequency differed significantly between *A. equina* with red/orange pedal discs and those with green pedal discs, consistent with the hypothesis that these morphotypes represent incipient species.

Introduction:

The Cnidarian genus *Actinia* (Cnidaria: Anthozoa: Actinaria: Actiniidae) is notably diverse, phenotypically variable and has had a fluid taxonomical history (Perrin et al., 1999). The beadlet anemone, *Actinia equina* is a common organism of North Atlantic rocky shores but has a reported range from the Kola Peninsula of northern Russia to the coast of South Africa (Manuel, 1988; Stephenson, 1935). Additionally, populations of *Actinia* in the Adriatic, Mediterranean and Black Sea (Schama et al., 2005; Schmidt, 1971) have been ascribed to *A. equina*, as have animals from the coasts of Japan (Honma et al., 2005; Yanagi et al., 1999), Korea (Song, 1984) and Hong Kong (Morton and Morton, 1983). Allozyme electrophoresis studies have suggested that *Actinia* from some geographically distinct populations represent separate species, now labelled *A. schmidti* (Mediterranean), *A. cari* (Mediterranean), *A. sali* (Cape Verde), *A. nigropuncta* (Madeira) and an, as yet, unnamed form from South Africa (Monteiro et al., 1997; Perrin et al., 1999; Schama et al., 2005). Whether other populations of animals currently labelled as *A. equina* are misidentified cryptic species, or truly represent extensions to the known geographic range of this species, has not yet been assessed. Even within British populations of *Actinia equina*, the tremendous diversity in colour of *Actinia* individuals has led to taxonomic confusion. Allozyme electrophoresis studies have demonstrated the specific status of the strawberry anemone *A. fragacea* (Carter and Thorpe, 1981) and suggested that the green-columned form is a separate species from *A. equina*, now labelled *A. prasina* (Sole-Cava and Thorpe, 1987) although see Schama et al. (2005), but additional cryptic species perhaps also exist, particularly those morphotypes that differ in the colour of the pedal disc (grey/green versus red/pink/orange). These morphotypes show clear differences in intertidal distribution (red/pink morphs are found higher up the shore with green/grey morphs lower down the intertidal zone) and have been shown to present diagnostic allozyme genotypes at both malate dehydrogenase and hexokinase loci (Quicke and Brace, 1984; Quicke et al., 1983). In addition, they exhibit significant differences in aggression, nematocyst morphology, adhesion, and settlement patterns (Brace and Reynolds, 1989; Collins et al., 2017; Perrin et al., 1999; Quicke and Brace, 1984;

Quicke et al., 1983; Quicke et al., 1985; Watts and Thorpe, 1998). *Actinia* remains a key and common ecological species within the intertidal zone (Collins et al., 2017; Perrin et al., 1999; Schama et al., 2005) and hence accurate understanding of its taxonomy and the ability to identify species is important for understanding the functional ecology of this environment.

Due to the taxonomic confusion surrounding this genus and the difficulties in applying morphological taxonomy to such soft-bodied animals, the study of mitochondrial DNA may aid in resolution of this problematical taxon. Whilst there is an increasing number of complete mitochondrial genomes from the phylum e.g. (Beagley et al., 1998; Chi et al., 2018; Foox et al., 2016; Zhang and Zhu, 2017), none is currently available from the genus *Actinia*. Application of mitochondrial DNA barcoding (Ratnasingham and Hebert, 2007) also seems a promising tool. However, the evolutionary rate of mtDNA in Cnidaria is considered to be low (Huang et al., 2008; Shearer et al., 2002) potentially presenting difficulties for the application of this methodology. DNA barcoding relies on the use of standard primers which for metazoans are typically those of Folmer et al. (1994) which target the *cytochrome oxidase subunit I* gene. However, the utility of *COI*, and whether other regions of the mtDNA molecule harbour more variation, remains untested.

As part of a study to generate a full reference genome for *A. equina* to facilitate investigation of the genomic basis of differentiation among beadlet anemone morphotypes, the complete mitochondrial genome of *Actinia equina* is reported here and the utility of mitochondrial DNA barcoding for studying intraspecific variation of British populations assessed.

Materials and Methods:

A single specimen of *Actinia equina* (with a red column and red pedal disc) was collected from Rhosneigr, Anglesey, North Wales, UK and kept in artificial seawater at 8°C for two weeks to allow it to purge of any food which may have contaminated extracted DNA. Prior to DNA extraction, the animal was inspected to ensure that there were no intra-gastrovascular cavity brooded offspring which may have introduced additional haplotypes into the extracted DNA (although evidence to

87 date suggests these would be clonal (Pereira et al., 2017)). It was then minced with a scalpel and
88 ground under liquid nitrogen. The resultant powder was added to 20ml 80 mM EDTA (pH 8.0), 100
89 mM Tris-HCl (pH 8.0), 0.5% SDS, 100 µg/mL proteinase K, and 40µl RNaseA (100mg/ml) and
90 incubated at 60°C for 3 hours. Genomic DNA was isolated from this solution by salt-chloroform
91 extraction (Müllenbach et al., 1989), precipitated with 0.6 volumes of isopropanol, and dissolved in
92 water. Extracted DNA was further purified using a Qiagen Genomic Tip 20/G following the
93 manufacturer's instructions and precipitated a second time with 0.6 volumes of isopropanol.
94 20kb-insert PacBio sequencing libraries were produced and sequenced on 5 SMRT cells on a Pacific
95 Biosciences Sequel (Pacific Biosciences, Menlo Park, CA, USA) at the Centre for Genomic Research,
96 University of Liverpool.
97 Sequencing produced 3,507,426 'polymerase reads' (single reads that can cover the same insert
98 multiple times) that were split into a total of 4,936,001 subreads (full or partial passes of the same
99 insert). Of these subreads, 487,629 were longer than 20 kb and 1,409,598 longer than 10 kb.
100 All subreads were assembled using CANU v1.7 (Koren et al., 2017) with default parameters for
101 PacBio data. To identify mitochondrial DNA, all assembled contigs were used to make a BLAST
102 database using BLAST+ v2.2.28 (Camacho et al., 2009). This was queried using BLASTn with two
103 published *A. equina* mitochondrial genes: a partial cytochrome B-like gene (*cytB*; GenBank accession
104 **DQ683369.1**) and a sequence containing the *cytochrome oxidase subunit I* gene (*COI*) and *homing*
105 *endonuclease* gene (*HEG*) (GenBank accession **DQ831335.1**). To check for errors in the final
106 mitochondrial genome sequence, all subreads were aligned to the sequence using bwa v0.7.12-
107 r1039 (Li and Durbin, 2009), using the bwa-mem algorithm with default parameters.
108 Initial annotation of mitochondrial genome features used MITOS (Bernt et al., 2013) with manual
109 annotation conducted to finalise gene models. tRNA genes identified by MITOS were further
110 investigated using tRNAscan (Lowe and Chan, 2016). Gene order was depicted using MTVIZ
111 (http://pacosy.informatik.uni-leipzig.de/mtviz) and G/C content depicted with CGView (Stothard and
112 Wishart, 2005). Sequence divergence between the mitochondrial genomes of *A. equina* and *A. viridis*

(accession number **KY860669**) was estimated for a 500 bp sliding window, moving in steps of 25 bp across the mitochondrial genome, using DNASp v6 (Rozas et al., 2017).

DNA barcoding

A. equina (*N* = 43) and *A. prasina* (*N* = 3) were collected from a range of locations around the UK and the Isle of Man (Table 1) leaving at least 2m between samples from the same shore to avoid sampling clones. DNA was extracted from tentacle samples using a GeneJet Genomic DNA extraction kit (ThermoFisher, UK). Partial *COI* fragments were amplified using the primers of Folmer et al. (1994) at 0.2µM using 1x GoTaq HS mastermix (Promega) with cycling conditions of 95°C for 3 min followed by 35 cycles of 95°C for 1 min, 40°C for 1 min, and 72°C for 1.5 mins, followed by a final extension step at 72°C for seven minutes. Alternative primers were used to amplify a 559bp section of the intergenic region between *COIII* and *COI* (5'-cgggttttcatggtctgcat-3' and 5'-ccaggggcagataactccaa-3') and a 598bp region between *COI* and *ND4* (5'-ccccgcctttgtctcatact-3' and 5'-caccataattgccagcccaa-3'), designed using Primer3 (Untergasser et al., 2012). PCRs were undertaken using 1x GoTaq HS mastermix with cycling conditions of 5 min at 94°C followed by 35 cycles of 94°C for 30 sec, 55°C for 30 sec and 72°C for 1 min and a final extension time of 72°C for 5 min with PCR products purified using a GeneJet PCR purification kit and sequenced by GATC Biotech, Konstanz, Germany. Sequences were aligned using ClustalW (Larkin et al., 2007).

Results

Both BLASTn searches (with default parameters) returned a single contig (41,948 bp) but each query sequence aligned to the contig more than once (which can occur when a circular sequence is assembled). The first position of the *cytB* sequence (positions 6,928 and 27,619 in tig00010800) was used to trim the contig into a full-length putative mitochondrial genome of 20,690 bp which was then reoriented with the first base of *ND5* at base 1. 8,996 subreads could be aligned back to this sequence with a median coverage depth of 2,044.

This genome contains the standard 13 protein coding genes typical of the mitochondrial DNA, two ribosomal subunits (small and large) and, in line with other Cnidarian genomes, just two transfer RNAs (tryptophan and methionine) (Figure 1). In addition, an open reading frame (*OrfA*) potentially encoding a 645 amino acid protein was located between *COII* and *ND4*. As for other Cnidaria, type I introns were found within *ND5* (with *ND1* and *ND3* within the intron) and *COI* (containing a truncated *homing endonuclease* gene (*HEG*) ORF). The *HEG* of *A. equina* has an ORF of 343 amino acids, slightly longer than that of *A. viridis* (339 amino acids). This is due to a single base insertion relative to the ORF of *A. viridis*, with a 6 base poly-A tract at positions 17,646-17,651 at which *A. viridis* has a 5bp poly-A tract. The insertion was confirmed by Sanger sequencing of PCR products. The region between *ND3* and *ND5* displayed a partial ORF with similarities to *ND5* and it appears likely that this is pseudogenic. The mitochondrial genome was 61.02% A/T although this varied across the genome (Figure 1). The complete sequence has been deposited in Genbank with accession number **MH545699**.

Sequencing of PCR amplicons of the standard barcoding region of *COI* using the primers of Folmer et al. (1994) showed that beadlet anemone samples collected from England, Scotland, Wales and the Isle of Man displayed only two haplotypes (Table 1, Figure 2) which differed by just 1bp, a G-A synonymous transition at position 16,941 (Haplotype A accession number: **MH636618**; Haplotype B accession number: **MH636619**). Whilst variation was low, haplotype A was only ever seen in *A. equina* with red or orange pedal discs and never in animals with green pedal discs or in *A. prasina* and this association between haplotype and *A. equina* colour morph was significant ($\chi^2 = 16.43$; $P < 0.0001$).

Sliding window analysis comparing the complete *A. equina* mitochondrial genome to the complete mitochondrial genome of *Anemonia viridis* revealed low sequence divergence, with the exception of the intergenic regions separating *COIII* and *COI*, and between *COI* and *ND4* (Figure 3). Using primers designed to amplify these regions of maximum interspecific divergence then, as for *COI*, intraspecific variation among *A. equina* in these regions was low with a single haplotype in the intergenic

fragment between *COI* and *ND4* (accession number **MH686230**) and just two haplotypes (accession numbers **MH686231**-**MH686232**), differing by two base pairs, for the fragment between *COIII* and *COI* (an A-T transversion at position 16,432 resulting in an I-L amino acid change in *COIII* and an intergenic C-T transition at 16,517).

Discussion

The mitochondrial genome of *Actinia equina* has the standard mitochondrial gene order typical of Cnidaria (Beagley et al., 1998; Chi et al., 2018; Foox et al., 2016) although at 20,690bp the mtDNA is slightly longer than that of other Cnidaria, largely due to an increased intergenic region between *ND3* and the second exon of *ND5*. This region contains a partial pseudogene of *ND5* as seen also in *Bolocera tuediae* (Emblem et al., 2014). As in *A. viridis* (Chi et al., 2018), the homing endonuclease gene of *A. equina* is fused in-frame with *COI* (Chi et al. 2018) but differs at the 3' end due to an insertion in a poly-A tract resulting in a frameshift.

Whole mitochondrial DNA sequences have been used to study Cnidarian phylogeny e.g. (Emblem et al., 2014; Foox et al., 2016) but individual mitochondrial genes are often used in studies of phylogenetics and population studies with the *cytochrome oxidase subunit I* the most common target. Here, sequencing of *COI* from *A. equina* samples collected from Scotland, Wales, England and the Isle of Man, and including individuals of *A. prasina* deemed a separate species based on allozyme evidence (Sole-Cava and Thorpe, 1987), detected only two haplotypes differing by just one base pair. *A. prasina* shared the same haplotype as *A. equina* with a green pedal disc. It seems therefore that the low variability of *COI* makes this gene of little use for population genetic studies. However, the fact that haplotype A was seen only in animals with red/orange pedal discs, and never in those with green pedal discs adds weight to the argument that these may represent incipient species (Collins et al., 2017; Perrin et al., 1999; Quicke et al., 1983). This low variability of mitochondrial DNA has been seen previously: Pereira et al. (2014), studying the mitochondrial *16S* gene, found only two haplotypes among 77 anemones from the coast of Portugal. It is extremely surprising that in a

191 species considered largely to reproduce through budding, and in which little evidence of sexual
192 reproduction has been found (Perrin et al., 1999), there is such a dearth of variability in the
193 mitochondrial genome across large geographic scales. In addition, the lack of difference in sequence,
194 or haplotype frequency, between *A. equina* and *A. prasina* is surprising. However, allozyme studies
195 of genetic distance find levels appropriate for interspecific comparisons when *A. prasina* is compared
196 to *A. equina* with a red pedal disc, but not when compared to samples with a grey pedal disc
197 (Schama et al., 2005) further suggesting that what is currently regarded as *A. equina* encompasses at
198 least two cryptic species. Other mitochondrial genes may be more variable and hence of more utility
199 for population genetics/phylogenetics. Emblem et al. (2014) demonstrated in interspecific
200 comparisons that of the protein coding complement of the mtDNA the *HEG* has the highest
201 evolutionary rate. However, previous work showed no intraspecific variation in the *HEG* sequence
202 when 95 individuals of the Anthozoan *Metridium senile* were compared (Goddard et al., 2006).
203 Intergenic regions of the mtDNA which are likely less constrained by selection pressures may be of
204 use and we show through comparison of sequence divergence between *A. equina* and *A. viridis*
205 across the whole molecule that two intergenic regions of the mitochondrial genome have maximum
206 divergence and hence hold promise as phylogenetic and population genetic markers. However, we
207 show through sequencing of *A. equina* and *A. prasina* individuals that within these species there are
208 few variable positions within these two regions, so they are of no more utility than the *COI*
209 barcoding region. Taken together, this suggests that the low inherent mutation rate of this molecule
210 make it uninformative for understanding the complex relationships within this genus or the
211 population genetics of the inherent species, and that nuclear DNA studies will instead need to be
212 conducted. Nevertheless, the significant difference in haplotype frequencies between red/orange
213 and green pedal disc anemones does add to the growing evidence from aggression, nematocyst
214 morphology, distribution and allozyme data (Collins et al., 2017; Perrin et al., 1999; Quicke et al.,
215 1983) that these may be incipient species. The causes of speciation in intertidal organisms have been
216 most intensively studied in the rough periwinkle *Littorina saxatilis* where 'crab' and 'wave'

morphotypes appear to be selected by the action of predator pressure (from crabs) and wave action (Butlin et al., 2014) and the genomic regions under selection are now being revealed (Westram et al., 2018). Wave action appears also to be a factor in speciation in other organisms, e.g. kelp (Augyte et al., 2018). However, the intertidal zone is characterized by a range of strong divergent selective pressures, both biotic and abiotic and such extreme stresses (as those imposed on intertidal organisms) can be sufficient to promote speciation (Lexer and Fay, 2005). The fact that anemones with red/orange pedal discs are found higher up the intertidal zone than those with green pedal discs (Perrin et al., 1999; Quicke and Brace, 1984; Quicke et al., 1983), and that differences are present in adhesion strength and preference for substratum orientation, with red pedal disc forms preferring more vertical surfaces than the green pedal disc form (Quicke and Brace, 1984; Quicke et al., 1983), indicates that ecological factors may indeed be driving speciation. In other Cnidarians ecological specialization is a driver of speciation (González et al., 2018) and this may also be the case for *Actinia*. The precise nature of the selective pressures on anemone populations remain to be elucidated but the availability of genetic and genomic resources (Wilding and Weedall, unpublished) for this widely-studied species will greatly aid in our efforts to understand the extent and pattern of differentiation in this ecologically important animal.

Acknowledgments

This work was supported by an award from the Liverpool John Moores University – Technology Directorate Voucher Scheme providing access to University of Liverpool's Shared Research Facilities. We thank Jeremy Hussey and John Halsall for assistance in the collections from the Isle of Man and Stefano Mariani for help with the Pembrokeshire collections.

References

241 Augyte, S., Lewis, L., Lin, S., Neefus, C.D., Yarish, C., 2018. Speciation in the exposed intertidal zone:
242 the case of *Saccharina angustissima comb. nov*. & *stat. nov*. (Laminariales, Phaeophyceae).
243 Phycologia 57, 100-112.
244 Beagley, C.T., Okimoto, R., Wolstenholme, D.R., 1998. The mitochondrial genome of the sea
245 anemone *Metridium senile* (Cnidaria): introns, a paucity of tRNA genes, and a near-standard genetic
246 code. Genetics 148, 1091-1108.
247 Bernt, M., Donath, A., Jühling, F., Externbrink, F., Florentz, C., Fritzsch, G., Pütz, J., Middendorf, M.,
248 Stadler, P.F., 2013. MITOS: Improved de novo metazoan mitochondrial genome annotation. Mol.
249 Phylogenet. Evol. 69, 313-319.
250 Brace, R.C., Reynolds, H.A., 1989. Relative intraspecific aggressiveness of pedal disc colour
251 phenotypes of the beadlet anemone, *Actinia equina*. J. Mar. Biol. Assoc. U.K. 69, 273-278.
252 Butlin, R.K., Saura, M., Charrier, G., Jackson, B., André, C., Caballero, A., Coyne, J.A., Galindo, J.,
253 Grahame, J.W., Hollander, J., Kemppainen, P., Martínez-Fernández, M., Panova, M., Quesada, H.,
254 Johannesson, K., Rolán-Alvarez, E., 2014. Parallel evolution of local adaptation and reproductive
255 isolation in the face of gene flow. Evolution 68, 935-949.
256 Camacho, C., Coulouris, G., Avagyan, V., Ma, N., Papadopoulos, J., Bealer, K., Madden, T.L., 2009.
257 BLAST+: architecture and applications. BMC Bioinformatics 10, 421.
258 Carter, M.A., Thorpe, J.P., 1981. Reproductive, genetic and ecological evidence that *Actinia equina*
259 var. *mesembryanthemum* and var. *fragacea* are not conspecific. J. Mar. Biol. Assoc. U.K. 61, 79-93.
260 Chi, S.I., Urbarova, I., Johansen, S.D., 2018. Expression of homing endonuclease gene and insertion-
261 like element in sea anemone mitochondrial genomes: Lesson learned from *Anemonia viridis*. Gene
262 652, 78-86.
263 Collins, J.R., Vernon, E.L., Thomson, J.S., 2017. Variation in risk-taking and aggression in morphotypes
264 of the beadlet anemone, *Actinia equina* (L.), and the green anemone, *Actinia prasina* (Gosse). J. Exp.
265 Mar. Biol. Ecol. 496, 29-36.

Emblem, Å., Okkenhaug, S., Weiss, E.S., Denver, D.R., Karlsen, B.O., Moum, T., Johansen, S.D., 2014. Sea anemones possess dynamic mitogenome structures. Mol. Phylogenet. Evol. 75, 184-193.

Folmer, O., Black, M., Hoeh, W., Lutz, R., Vrijenhoek, R., 1994. DNA primers for the amplification of mitochondrial *cytochrome oxidase subunit I* from diverse metazoan invertebrates. Mol. Mar. Biol. Biotechnol. 3, 294-299.

Foox, J., Brugler, M., Siddall, M.E., Rodríguez, E., 2016. Multiplexed pyrosequencing of nine sea anemone (Cnidaria: Anthozoa: Hexacorallia: Actiniaria) mitochondrial genomes. Mitochondrial DNA Part A 27, 2826-2832.

Goddard, M.R., Leigh, J., Roger, A.J., Pemberton, A.J., 2006. Invasion and persistence of a selfish gene in the Cnidaria. PLoS ONE 1, e3.

González, A.M., Prada, C.A., Ávila, V., Medina, M., 2018. Ecological speciation in corals, in: Oleksiak, M.F., Rajora, O.P. (Eds.), Population Genomics: Marine Organisms. Springer.

Honma, T., Minagawa, S., Nagai, H., Ishida, M., Nagashima, Y., Shiomi, K., 2005. Novel peptide toxins from acrorhagi, aggressive organs of the sea anemone *Actinia equina*. Toxicon 46, 768-774.

Huang, D., Meier, R., Todd, P.A., Chou, L.M., 2008. Slow mitochondrial CoI sequence evolution at the base of the metazoan tree and its implications for DNA barcoding. J. Mol. Evol. 66, 167-174.

Koren, S., Walenz, B.P., Berlin, K., Miller, J.R., Bergman, N.H., Phillippy, A.M., 2017. Canu: scalable and accurate long-read assembly via adaptive *k*-mer weighting and repeat separation. Genome Res. 27, 722-736.

Larkin, M.A., Blackshields, G., Brown, N.P., Chenna, R., McGettigan, P.A., McWilliam, H., Valentin, F., Wallace, I.M., Wilm, A., Lopez, R., Thompson, J.D., Gibson, T.J., Higgins, D.G., 2007. Clustal W and Clustal X version 2.0. Bioinformatics 23, 2947-2948.

Lexer, C., Fay, M.F., 2005. Adaptation to environmental stress: a rare or frequent driver of speciation? J. Evol. Biol. 18, 893-900.

Li, H., Durbin, R., 2009. Fast and accurate short read alignment with Burrows–Wheeler transform. Bioinformatics 25, 1754-1760.

292 Lohse, M., Drechsel, O., Kahlau, S., Bock, R., 2013. OrganellarGenomeDRAW—a suite of tools for
293 generating physical maps of plastid and mitochondrial genomes and visualizing expression data sets.
294 Nucleic Acids Res. 41, W575-W581.
295 Lowe, T.M., Chan, P.P., 2016. tRNAscan-SE On-line: integrating search and context for analysis of
296 transfer RNA genes. Nucleic Acids Res. 44, W54-W57.
297 Manuel, R.L., 1988. British Anthozoa. E.J. Brill, Leiden.
298 Monteiro, F.A., Solé-Cava, A.M., Thorpe, J.P., 1997. Extensive genetic divergence between
299 populations of the common intertidal sea anemone *Actinia equina* from Britain, the Mediterranean
300 and the Cape Verde Islands. Marine Biology 129, 425-433.
301 Morton, B., Morton, J., 1983. The sea shore ecology of Hong Kong. Hong Kong: Hong Kong.
302 Müllenbach, R., Lagoda, P.J., Welter, C., 1989. An efficient salt-chloroform extraction of DNA from
303 blood and tissues. Trends Genet. 5, 391.
304 Pereira, A.M., Brito, C., Sanches, J., Sousa-Santos, C., Robalo, J.I., 2014. Absence of consistent genetic
305 differentiation among several morphs of *Actinia* (Actiniaria: Actiniidae) occurring in the Portuguese
306 coast. Zootaxa 3893, 595-600.
307 Pereira, A.M., Cadeireiro, E., Robalo, J.I., 2017. Asexual origin of brooding in the sea anemones
308 *Actinia equina* and *A. schmidti*: molecular evidence from the Portuguese shore. N. Z. J. Mar. Freshw.
309 Res. 51, 316-320.
310 Perrin, M.C., Thorpe, J.P., Solé-Cava, A.M., 1999. Population structuring, gene dispersal and
311 reproduction in the *Actinia equina* species group. Oceanography and Marine Biology 37, 129-152.
312 Quicke, D.L.J., Brace, R.C., 1984. Evidence for the existence of a third, ecologically distinct morph of
313 the anemone, *Actinia equina*. J. Mar. Biol. Assoc. U.K. 64, 531-534.
314 Quicke, D.L.J., Donoghue, A.M., Brace, R.C., 1983. Biochemical-genetic and ecological evidence that
315 red/brown individuals of the anemone *Actinia equina* comprise two morphs in Britain. Mar. Biol. 77,
316 29-37.

317 Quicke, D.L.J., Donoghue, A.M., Keeling, T.F., Brace, R.C., 1985. Littoral distributions and evidence for
318 differential post-settlement selection of the morphs of *Actinia equina*. J. Mar. Biol. Assoc. U.K. 65, 1-
319 20.
320 Ratnasingham, S., Hebert, P.D.N., 2007. BOLD: The Barcode of Life Data System
321 (http://www.barcodinglife.org). Mol. Ecol. Notes 7, 355-364.
322 Rozas, J., Ferrer-Mata, A., Sánchez-DelBarrio, J.C., Guirao-Rico, S., Librado, P., Ramos-Onsins, S.E.,
323 Sánchez-Gracia, A., 2017. DnaSP 6: DNA sequence polymorphism analysis of large data sets. Mol.
324 Biol. Evol. 34, 3299-3302.
325 Schama, R., Solé-Cava, A.M., Thorpe, J.P., 2005. Genetic divergence between east and west Atlantic
326 populations of *Actinia* spp. sea anemones (Cnidaria: Actiniidae). Marine Biology 146, 435-443.
327 Schmidt, H., 1971. Taxonomie, verbreitung und variabilität von *Actinia equina* Linnt 1766 (Actiniaria;
328 Anthozoa). Zeitschrift für Zoologische Systematik und Evolutionsforschung 9, 161-169.
329 Shearer, T.L., van Oppen, M.J.H., Romano, S.L., Wörheide, G., 2002. Slow mitochondrial DNA
330 sequence evolution in the Anthozoa (Cnidaria). Mol. Ecol. 11, 2475-2487.
331 Sole-Cava, A.M., Thorpe, J.P., 1987. Further genetic evidence for the reproductive isolation of green
332 sea anemone *Actinia prasina* Gosse from common intertidal beadlet anemone *Actinia equina* (L.).
333 Mar. Ecol. Prog. Ser. 38, 225-229.
334 Song, J.-I., 1984. A systematic study on the Korean Anthozoa. 8. Actiniaria (Hexacorallia). J. Korean
335 Res. Inst. Better Living 34, 69-88.
336 Stephenson, T.A., 1935. The British sea anemones. The Ray Society, London.
337 Stothard, P., Wishart, D.S., 2005. Circular genome visualization and exploration using CGView.
338 Bioinformatics 21, 537-539.
339 Untergasser, A., Cutcutache, I., Koressaar, T., Ye, J., Faircloth, B.C., Remm, M., Rozen, S.G., 2012.
340 Primer3 - new capabilities and interfaces. Nucleic Acids Res. 40, e115.

341 Watts, P.C., Thorpe, J.P., 1998. Phenotypic identification of three genetically differentiated morphs
342 of the intertidal beadlet anemone *Actinia equina* (Anthozoa: Cnidaria). J. Mar. Biol. Assoc. U.K. 78,
343 1365-1368.
344 Westram, A.M., Rafajlović, M., Chaube, P., Faria, R., Larsson, T., Panova, M., Ravinet, M., Blomberg,
345 A., Mehlig, B., Johannesson, K., Butlin, R., 2018. Clines on the seashore: the genomic architecture
346 underlying rapid divergence in the face of gene flow. Evol. Letters 2, 297-309.
347 Yanagi, K., Segawa, S., Tsuchiya, K., 1999. Early development of young brooded in the enteron of the
348 beadlet sea anemone *Actinia equina* (Anthozoa: Actiniaria) from Japan. Invertebrate Reproduction &
349 Development 35, 1-8.
350 Zhang, L., Zhu, Q., 2017. Complete mitochondrial genome of the sea anemone, *Anthopleura midori*
351 (Actiniaria: Actiniidae). Mitochondrial DNA Part A 28, 335-336.
352
353 **Figure Legends:**
354 Figure 1:
355 Gene order in *Actinia equina* mitochondrial DNA (20,690bp). Figure produced in MTVIZ
356 (http://pacosy.informatik.uni-leipzig.de/mtviz). %AT is shown within the gene order diagram. Grey
357 shaded areas indicate intergenic regions.
358 Figure 2:
359 Collection sites for *Actinia equina* samples. For sample sizes refer to Table 1. The relative frequency
360 of the two haplotypes (Haplotype A: black; Haplotype B: light grey) is depicted in each pie chart. R =
361 red/orange pedal discs, G = green pedal discs, P = *A. prasina*.
362 Figure 3:
363 Sliding window analysis of the alignment of *Actinia equina* and *Anemonia viridis* mitochondrial
364 genomes. The line shows the value of nucleotide diversity (π) in a sliding window analysis of window
365 size 500 bp with step size 25 bp with the value plotted at its mid-point. Genes are displayed as grey

366 boxes below the x-axis. Genes with introns are labelled with *. Positions of amplified PCR products:

367 a) *COIII-COI* b) Folmer and c) *COI-ND4*. Figure drawn in OGDRAW (Lohse et al., 2013).

368 **Table 1: Haplotype distribution in geographic samples of *A. equina* and *A. prasina* from England,**

369 **Wales, Scotland and the Isle of Man. Only two haplotypes are found, Haplotype A (accession**

370 **MH636618) and Haplotype B (MH636619), differing by 1bp.**

		Haplotype A	Haplotype B
Millport, Isle of Cumbrae, Scotland	Green	0	2
	Orange	3	0
	Red	1	1
Peel, Isle of Man	Green	0	1
	Red	1	0
	A. prasina	0	1
Niarbyl, Isle of Man	Red	0	1
New Brighton, Wirral, England	Green	0	2
	Red	0	4
	A. prasina	0	2
Llandudno, North Wales	Green	0	2
	Red	2	0
Holyhead, Anglesey, North Wales	Green	0	3
	Red	2	0
Rhosneigr, Anglesey, North Wales	Green	0	2
	Red	2	0
St Brides Bay, South Wales	Green	0	4
	Red	2	2
Marloes, South Wales	Green	0	3
	Red	3	0

371

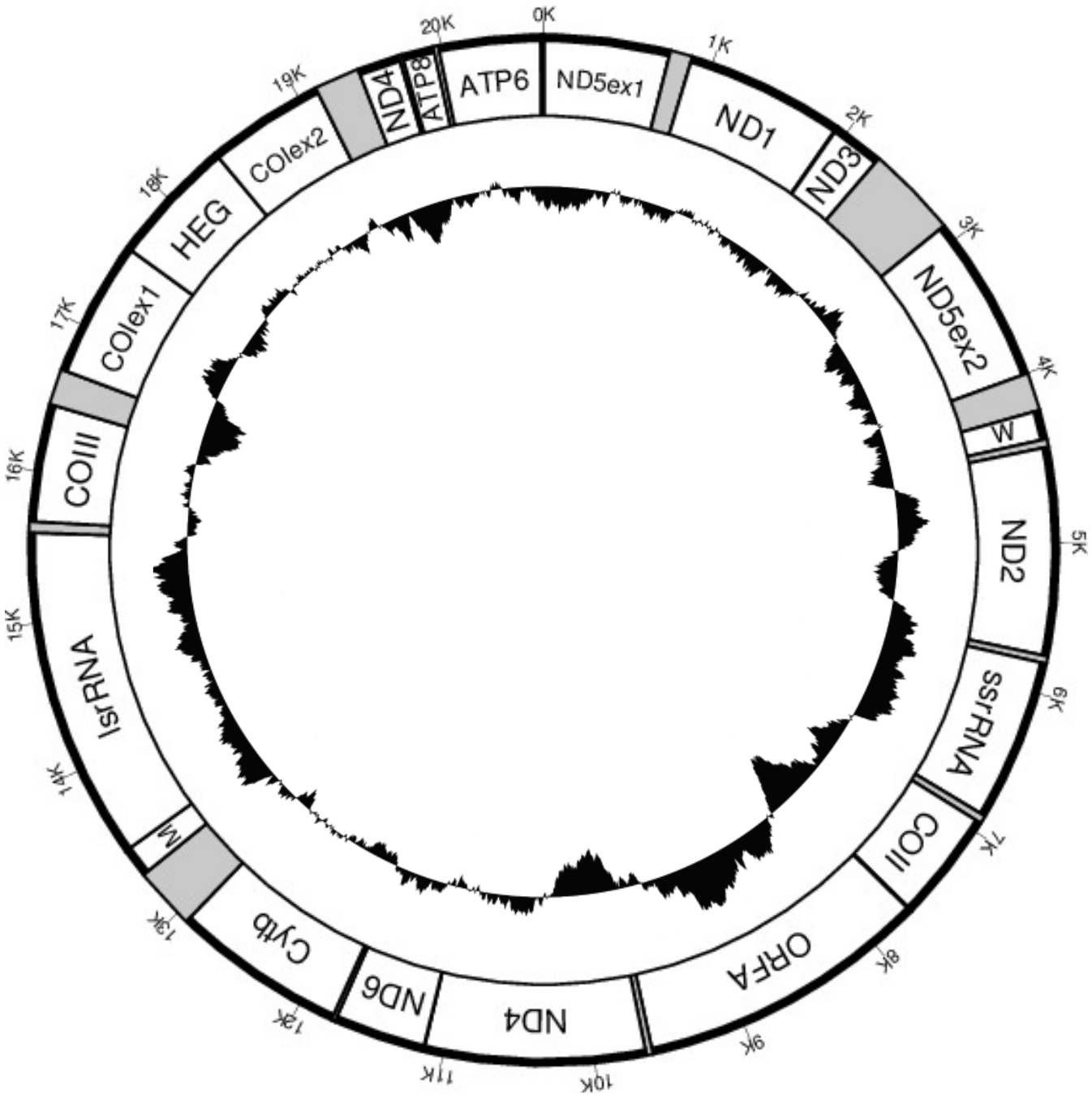
0K
1K
2K
3K
4K
5K
6K
7K
8K
9K
10K
11K
12K
13K
14K
15K
16K
17K
18K
19K
20K
ATP6
ATP8
ND4
ND5ex1
ND1
ND3
ND5ex2
W
ND2
ssrRNA
COII
ORFA
ND4
ND6
Cytb
M
lsrRNA
COIII
COIex1
HEG
COIex2

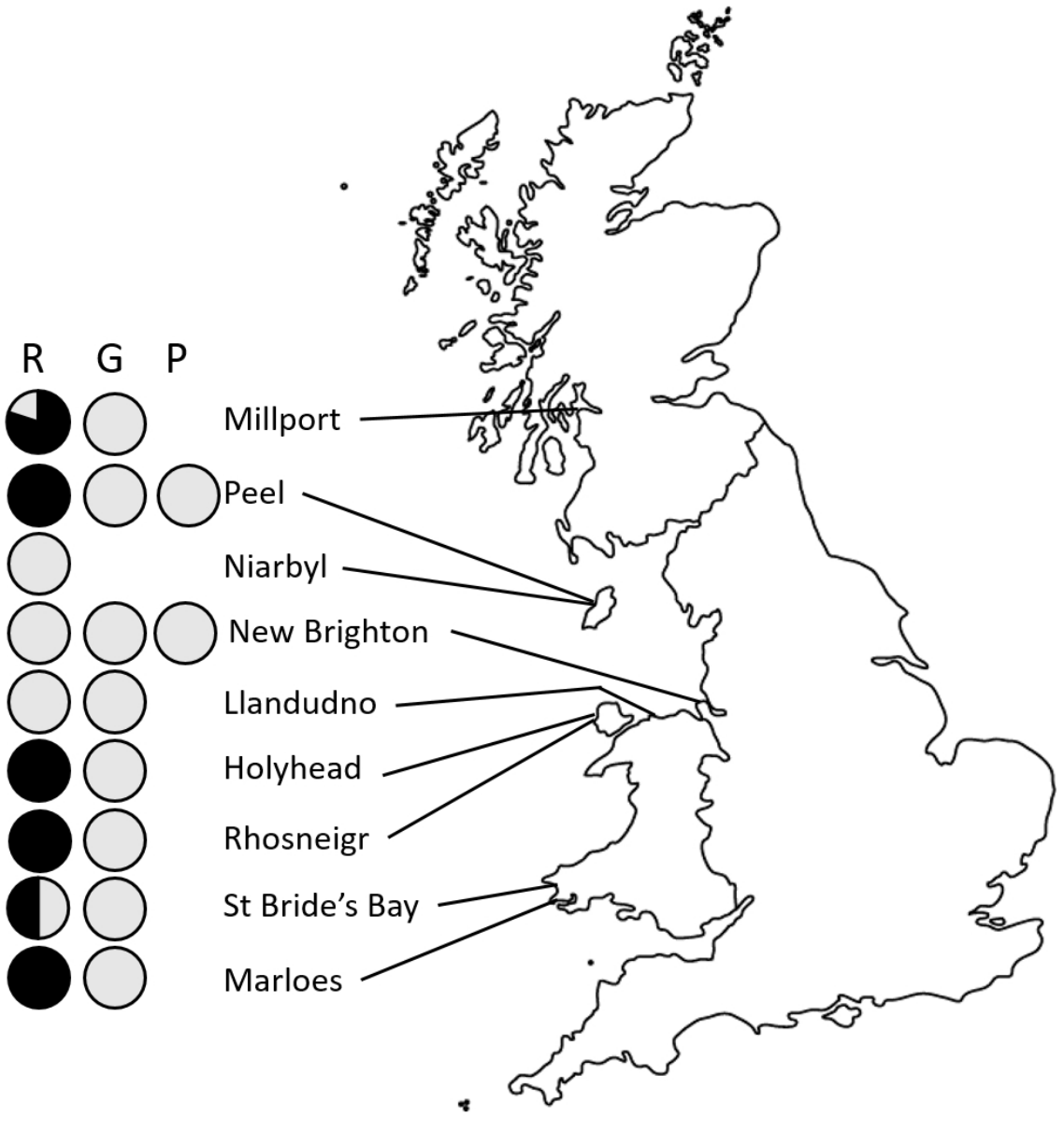
R
G
P
Millport
Peel
Niarbyl
New Brighton
Llandudno
Holyhead
Rhosneigr
St Bride's Bay
Marloes

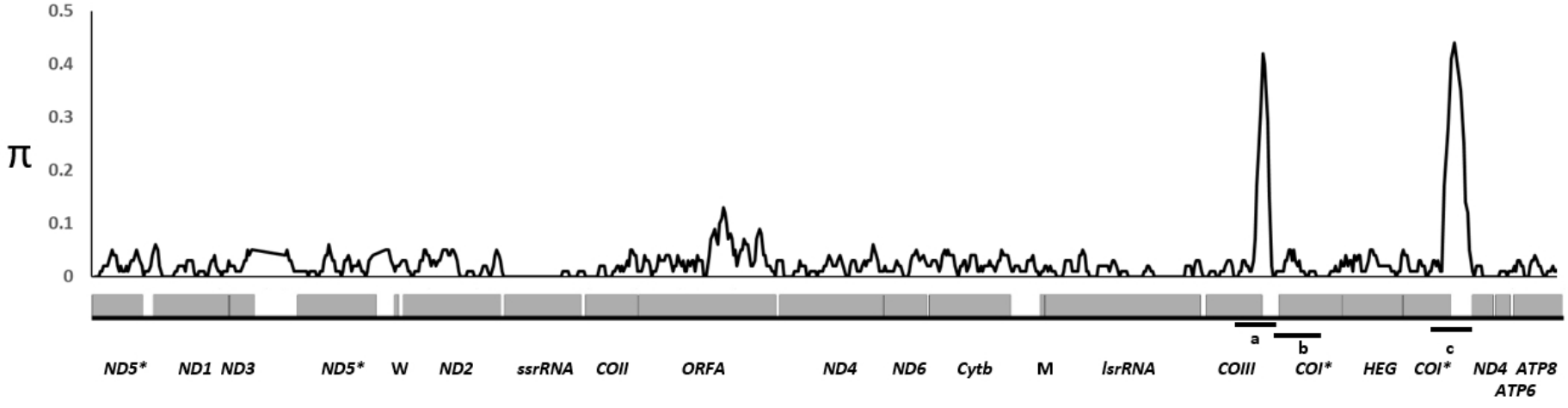
π
0.5
0.4
0.3
0.2
0.1
0
a
b
c
ND5*
ND1
ND3
ND5*
W
ND2
ssrRNA
COII
ORFA
ND4
ND6
Cytb
M
lsrRNA
COIII
COI*
HEG
COI*
ND4
ATP8
ATP6